

Microstructure of quenched and annealed films of isotactic polypropylene

Part I

N. ALBEROLA, M. FUGIER

Laboratoire Matériaux Composites, E.S.I.G.E.C., Université de Savoie, B.P. 1104, 73376 Le Bourget du Lac, France

D. PETIT, B. FILLON

Péchiney Centre de Recherches de Voreppe, Z. I. Centr'Alp, B.P. 27, 38340 Voreppe, France

The Microstructure of quenched and annealed iPP films was investigated by means of differential scanning calorimetry (DSC), density measurements, wide-angle X-ray diffraction (WAXD) and dynamic mechanical spectrometry (DMS). It was found that quenched iPP can be described as a biphasic material constituted of an amorphous phase strongly cross-linked by many crystalline entities exhibiting both small size and very low degree of perfection. Such microcrystallites act as true physical ties of the amorphous phase. On increasing the annealing temperature from 20 °C (quenched film) to 160 °C, the crystallinity ratio first remained constant for annealing temperatures between 20 and 93 °C and then it increased. Subsequently, both size and degree of perfection of crystalline entities progressively increased and tended towards the characteristics of the monoclinic phase. This resulted in a progressive decrease in the physical cross-linking degree of the amorphous phase, even for the samples exhibiting the highest crystallinity ratio.

1. Introduction

Isotactic polypropylene (PP) displays three well-known crystalline structures, namely, monoclinic (α form), hexagonal (β form) and triclinic (γ form) [1, 2]. The α form, the most stable and compact form, which predominates, is obtained under the usual crystallization conditions [2-4]. The β form is less prevalent and results from a particular crystallization mode, i.e. applied shear stress during processing [2, 5]. Finally, the γ form is the rarest and it is favoured by a low molecular weight of PP and high pressure [6-8].

Quenching the molten polymer leads to a phase exhibiting an intermediate crystalline order, the precise nature of which is still disputed in the literature. As the X-ray diffraction trace of quenched isotactic polypropylene film displays two broad and diffuse diffraction profiles, it is suggested that the quenched polymer is a two-phase system, i.e. amorphous and paracrystalline phases [9]. According to Miller [9] and Zannetti *et al.* [10], this paracrystalline phase is three-dimensionally ordered but with a high incidence of crystallographic defects. Alternatively, Bodor *et al.* [11], using X-ray techniques, suggest that the quenched form of isotactic polypropylene is composed of microcrystallites of monoclinic habit. Gezowich and Geil [12] agree with the microcrystallinity, but propose a hexagonal habit. According to McAllister *et al.* [13], this quenched form is composed of microcrystalline arrays of cubic or tetragonal symmetry.

From mathematical X-ray peak separation performed on quenched PP diffractograms, McAllister *et al.* [13] estimated the crystallite size of such a form to be about 3 nm. These results are in agreement with the crystallite size data of the paracrystalline phase of quenched PP reported by Hsu *et al.* [14] using electron microscopy. Other structural models have been proposed by Natta [15], regarding the quenched form of PP as a "frozen liquid" structure and sometimes described as a "smectic phase", and by Grebowicz *et al.* [16], considering the quenched form of isotactic polypropylene as a condensation crystal. From infrared experiments and X-ray diffraction analysis, Glotin *et al.* [17] and Hendra *et al.* [18] suggest that the quenched form of isotactic polypropylene is composed of rods of ordered helical molecules which are not coherent, i.e. they are not packed into developed three-dimensional crystalline micelles. According to Saraf and Porter [19], this smectic phase is formed by 3/1 helices highly oriented, but the lateral packing of such helices is highly disordered.

From a model of the X-ray diffraction pattern of quenched isotactic polypropylene film, Corradini *et al.* [20] agree with such a structural description of the mesomorphic phase. Moreover, these authors show that the local correlations between chains are probably nearer to those characterizing the crystal structure of the monoclinic form than to those characteristic of the structure of the hexagonal form.

The paracrystalline or smectic phase of isotactic polypropylene is relatively stable at room temperature for long periods of time but transforms into the monoclinic form when heated above 60 °C [10, 21–26]. Thus, it was suggested that, on annealing, there is a decrease in the amount of both the amorphous and the paracrystalline phases. Subsequently, the amount of monoclinic phase, the crystal size, and the degree of perfection are increased [24–26]. The transformation of the paracrystalline phase into the monoclinic form, occurring either on annealing samples at various temperatures or on isochronal scans, was analysed through various experimental techniques such as wide-angle X-ray diffraction (WAXD), density and sorption of dichloromethane vapour at low activity, and differential scanning calorimetry (DSC).

In the present work, the microstructure of quenched and annealed films of isotactic polypropylene (iPP) films was investigated through the analysis of both the crystalline phase and the magnitude of interactions between phases, i.e. the cross-linking degree of the amorphous phase by the crystalline entities. Thus, the crystalline phase characteristics of quenched and annealed films were analysed by using DSC, WAXD and density measurements.

The magnitude of interactions between phases was evaluated using dynamic mechanical spectrometry (DMS).

In Part II of this paper [27], the mechanical properties of these films are discussed in view of the microstructural analysis detailed in this paper.

2. Experimental procedure

2.1. Materials

Isotactic polypropylene used in this work has a given tactic purity of 97% and mean molecular weights $\overline{M}_n = 62\,000$ and $\overline{M}_w = 250\,000$. Sheets of quenched isotactic polypropylene films (iPP) with thicknesses of about 40 μm were provided by CRV Pechiney Company (France).

As-received films were annealed for 10 min at four temperatures, i.e. 70, 93, 135 and 160 °C. The as-received film is denoted Q, and the annealed samples A, followed by the annealing temperatures, i.e. A70, A93, A135 and A160.

2.2. Wide-angle X-ray diffraction (WAXD)

The wide-angle X-ray diffractograms of as-received and annealed samples were recorded at room temperature by using a Siemens D500 diffractometer ($\text{CuK}\alpha$, nickel-filtered radiation) with 0.02° (2 θ) scan increments.

2.3. Density

The density of as-received and annealed samples was evaluated by using a high-precision top-loading electronic Mettler balance. The density was determined by immersing the sample in a mixture of dodecane, the density of which is known.

The density of the sample was determined through the relationship

$$d = \frac{M_o}{M_o - M} d_{\text{dod}} \quad (1)$$

where M_o is the weight of the PP sample in air, M is the measured weight of PP sample immersed in dodecane, and d_{dod} is the density of the dodecane at the experimental temperature.

2.4. Differential scanning calorimetry (DSC)

Differential scanning calorimetry (DSC) was carried out over the temperature range from –30 to +200 °C using a Perkin–Elmer DSC 7 instrument purged with helium gas and chilled with liquid nitrogen. In general, about 10 mg samples of the quenched polypropylene film were used. DSC traces were recorded at different heating rates from 5–50 °C min^{–1}. Thermograms were calibrated by scanning melting-point substances, i.e. *n*-octadecane and indium, at the same heating rate. This allowed two corrections to the ordinate, both of which are essential for detailed comparisons to be made. One of these is the correction for thermal lag in the differential control loop obtained from the leading edge slope of indium and *n*-octadecane endotherm. The other, of particular interest when comparing different scan rates, is for thermal lag in the average control loop which adds directly to any error in the calibration. Baselines were determined by running an empty can at the same rate of the analysed samples, giving a curve which was subtracted from the specimen thermograms.

2.5. Dynamic mechanical spectrometry (DMS)

Dynamic mechanical experiments were performed on (10 × 5) mm² sheets of polypropylene films by using a Polymer Laboratories Dynamic Mechanical Tensile Analyser (DMTA) over the temperature range –50 to +100 °C at three frequencies, 1, 5 and 10 Hz. This set up provides the real, E' , and imaginary, E'' , parts of dynamic tensile modulus and $\tan \delta$ ($= E''/E'$) as functions of temperature for the three frequencies.

The aim of such an investigation was to analyse the dynamic mechanical behaviour of the amorphous phase in the glass temperature range of the quenched and annealed iPP films in order to evaluate the magnitude of interactions between phases.

3. Results and discussion

3.1. Differential scanning calorimetry (DSC)

Fig. 1 shows the thermograms of a quenched iPP film recorded on increasing the temperature at 5, 10, 20, 40 and 50 °C min^{–1}.

Melting points were calibrated by scanning melting-point substances, i.e. *n*-octadecane and indium at, respectively, the same scan rate. All thermograms exhibit three peaks defined as T_1 , T_2 and T_3 on increasing the temperature. Thus, the thermogram

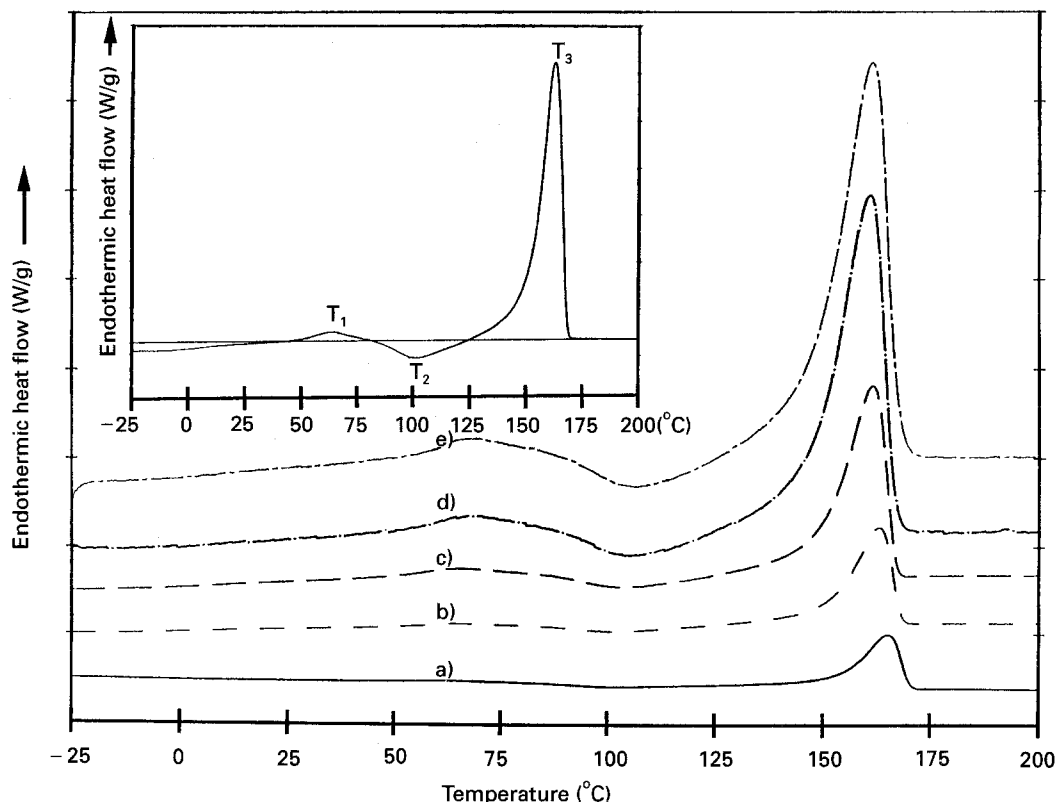


Figure 1 Thermograms of quenched iPP films recorded on increasing the temperature at the five following heating rates: (a) 5, (b) 10, (c) 20, (d) 40 and (e) 50 °C min⁻¹. Inset: an enlargement of the thermogram recorded at 10 °C min⁻¹.

TABLE I Characteristic values determined from thermograms recorded at various heating rates: (a) melting points are calibrated for each heating rate, (b) melting points are calibrated at the same heating rate (10 °C min⁻¹). T_1 , T_2 and T_3 are the temperature locations of the first endothermic peak, the exothermic maximum and the main upper endothermic peak, respectively

Heating rate (°C min ⁻¹)	(a) With calibration for each heating rate							(b) Without specific calibration						
	T_1 (°C)	ΔH_1 (J g ⁻¹)	T_2 (°C)	ΔH_2 (J g ⁻¹)	T_3 (°C)	ΔH_3 (J g ⁻¹)	X_c (%)	T_1 (°C)	ΔH_1 (J g ⁻¹)	T_2 (°C)	ΔH_2 (J g ⁻¹)	T_3 (°C)	ΔH_3 (J g ⁻¹)	X_c (%)
5	64	5 ± 2	99.5	-7 ± 2	165.0	92	67	48	2 ± 2	91.8	-9 ± 2	165.9	96	70
10	64	4 ± 2	101.5	-9 ± 2	162.6	83	60	64	4 ± 2	101.5	-9 ± 2	162.6	83	60
20	64	5 ± 2	103.2	-8 ± 2	161.3	83	60	66	8 ± 2	104.3	-6 ± 2	162.9	83	60
40	68	5 ± 2	105.4	-9 ± 2	160.5	79	57	70	9 ± 2	107.1	-6 ± 2	163.4	83	60
50	68	6 ± 2	106.2	-8 ± 2	161.1	78	57	73	7 ± 2	107.8	-7 ± 2	161.0	82	59

recorded at 10 °C min⁻¹ shows the three following transitions:

- (i) an endothermic peak (T_1) located in the temperature range 40–80 °C and centred at ca. 64 °C;
- (ii) an exothermic peak (T_2) ranging from 80–120 °C and centred at about 100 °C;
- (iii) a large endothermic peak (T_3) located at about 160 °C.

As both the first endothermic peak (T_1) and the exothermic peak (T_2) are not observed for isotactic polypropylene crystallized under the usual conditions, these peaks can be ascribed to specific phase transitions occurring in the quenched form of iPP. This is in agreement with the literature [14, 28].

In order to obtain evidence for the influence of the calibration conditions, Table I shows the characteristic values determined from thermograms at various

heating rates and calibrated for each scan rate compared to those determined without specific calibration. It can be noted that, without specific calibration, at any heating rate, the first endothermic peak (T_1), appears to be strongly shifted towards higher temperature with increasing scan rate, while it remains almost unchanged when specific calibration is used. Thus, the apparent rate dependence of such a transition could lead to the wrong conclusion about the origin of such an endothermic peak when no specific calibration is performed.

Accordingly, in agreement with Fichera and Zanetti [29], it can be concluded that T_1 , exhibiting no true heating-rate dependence, could be due to the melting of crystalline entities which show small size and/or low degree of perfection.

On increasing the heating rate from 5 °C min⁻¹ to 50 °C min⁻¹, the exothermic peak, T_2 , is shifted

towards higher temperature. Such a heating-rate dependence of T_2 , detected even for the lowest scan rates, suggests that this transition could result from a crystallization phenomenon which is a well-known thermally activated process, i.e. heating-rate dependent. This agrees with other reports [25, 26] which have related this exothermic process to a paracrystalline or smectic phase \rightarrow monoclinic form transition.

Because of the uncertainties in the precise determinations of both melting and crystallization enthalpies of these two transitions which appear very weak, it can be concluded that no significant changes in these values can be detected on increasing the scan rate.

The shift of the upper melting peak, T_3 , related to the melting of the thickest and more perfect crystallites of monoclinic habit towards the higher temperatures with decreasing the heating rate, suggests that some annealing occurs on heating. The subsequent increase in the crystallinity ratio observed with decreasing scan rate agrees with such a conclusion. Moreover, whatever the heating rate, no change in the slope of the baseline characteristic of the glass transition can be detected. This could suggest that the amorphous phase is strongly physically cross-linked by the crystalline entities in such a polymer.

Thus, quenched iPP films exhibit a double melting behaviour as do many other polymers, for example PEEK [30, 31], polyethylene [32, 33] and polyethylene oxide [34]. According to the literature [23–26, 35, 36], the complex melting behaviour of isotactic polypropylene could result from melting and recrystallization phenomena of initial microcrystallites or smectic phase developed on quenching. Such an interpretation is supported by many authors for numerous polymers [30, 37–40]. Then, quenched polypropylene film could be a two-phase system, i.e. amorphous–paracrystalline phase. According to this interpretation, the exothermic peak, T_2 , could be related to a recrystallization phenomenon of the original distorted crystallites.

According to this explanation, the crystallization enthalpy shown by the quenched polypropylene film on an isochronal run must be of the same order as the melting enthalpy of the lamellae of monoclinic habit. But, from enthalpy values reported in Table I, it can be seen that the enthalpy related to the melting of the thickest lamellae (ΔH_3) is about ten times higher than the crystallization enthalpy (ΔH_2), i.e. the energy is apparently not conserved, which is not consistent with the energy-conservation principle.

Such a difference between melting and crystallization enthalpies can be interpreted as follows.

(i) The as-received quenched polypropylene could not be a two but a three-phase system, i.e. amorphous–paracrystalline phase–monoclinic phase. According to the DSC experiments, the amount of monoclinic phase could be significantly higher than that of the paracrystalline phase. Thus, the double melting behaviour of quenched isotactic polypropylene films could be due to the presence of two initial populations

of crystallites, as was suggested for many other polymers [31, 32, 41] exhibiting a similar complex melting behaviour. But, the pattern of the X-ray diffractogram showing two broad reflection profiles (see after) is not consistent with the presence of a monoclinic form as the main phase. Then, this assumption, based on an initial three-phase system, could not be retained.

(ii) the apparent difference between the melting and crystallization enthalpy, exhibited by quenched polypropylene films on isochronal runs, could result from successive transitions which overlap on increasing the temperature. Thus, on an isochronal run, the less stable microcrystallites begin to melt from 40 °C. Such melting of the crystalline entities could induce a decrease in the cross-linking degree of the amorphous phase, i.e. molecular mobility is enhanced. Consequently, the crystallization resulting from the growth of the remaining microcrystallites could occur. Thus, with increasing temperature, the microcrystallites progressively melt, while almost simultaneously, new crystallites which are increasingly thicker and/or stable are formed.

Thus, the enthalpies of both the endotherm related to the melting of the microcrystallites and the crystallization exotherm determined from the area under each characteristic peak, are not truly representative of each transition considered separately. Such transitions, occurring almost simultaneously, overlap on increasing the temperature, leading to a minimization of their respective measured enthalpy. Moreover, some overlapping of melting and crystallization of the newly formed thickest lamellae, on increasing the temperature, could occur, leading again to a minimization of the observed crystallization peak area. Then, as the thickest and/or more perfect crystalline lamellae result from the crystallization process induced by the melting of the primary microcrystallites, the crystallinity index could be determined, as a first approximation, from the area under the main endothermic peak, T_3 , related to the melting of the newly formed crystallites on heating. For a scan rate of 10 °C min⁻¹, a crystallinity ratio of about 60% was found by using a melting enthalpy value of the monoclinic phase equal to 137 J g⁻¹ [33].

Fig. 2 shows the thermograms recorded at 10 °C min⁻¹ for samples annealed for 10 min at 70, 93, 135 and 160 °C. The thermogram of quenched iPP film is given as reference. Characteristic values of transitions are reported in Table II.

On increasing the annealing temperature from 20 °C (quenched sample) to 135 °C, the first endothermic peak (T_1) is strongly shifted towards the higher temperatures while the location of T_3 remains unchanged. The sample annealed at the highest temperature, i.e. 160 °C, exhibits only one endothermic peak (T_3) located at about 172 °C. Moreover, the crystallinity index is almost constant for samples annealed between 20 and 93 °C and then, it increases for samples annealed at 135 and 160 °C. Accordingly, with increasing annealing temperature, it is proposed that microcrystallites become increasingly thicker and/or stable leading to the observed shift of T_1 towards the

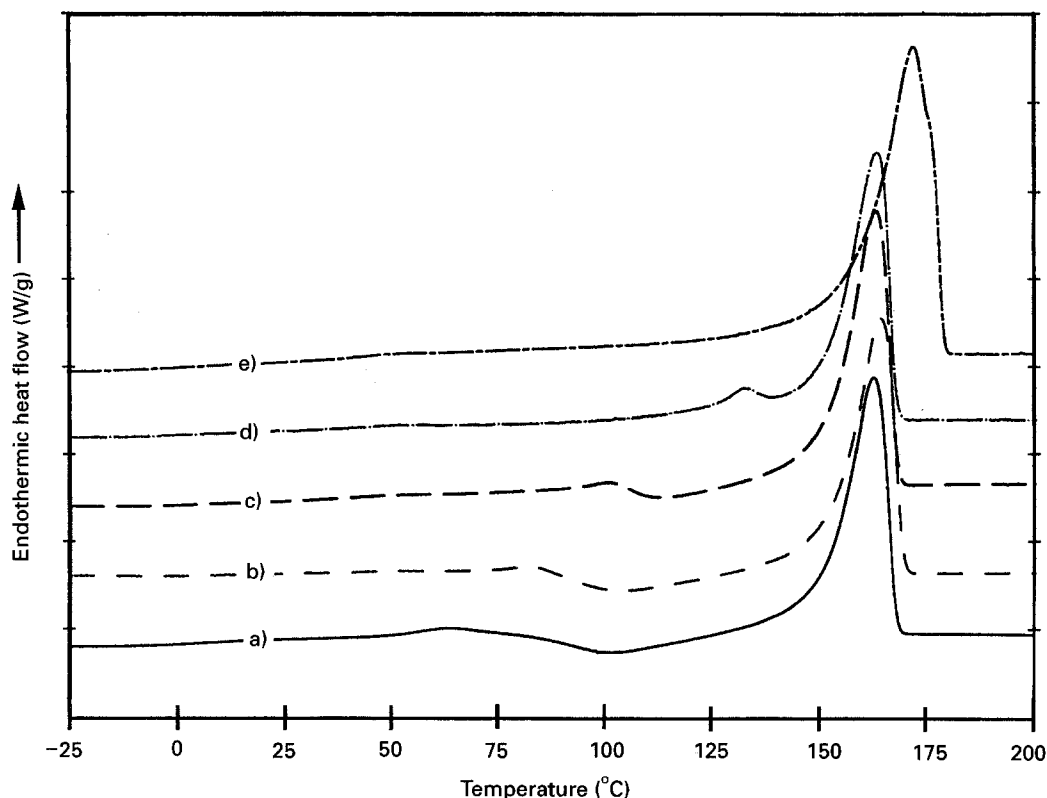


Figure 2 Thermograms recorded at $10^{\circ}\text{C min}^{-1}$ for (a) quenched iPP films, or samples annealed for 10 minutes at (b) 70°C , (c) 93°C , (d) 135°C and (e) 160°C .

TABLE II Characteristic values determined from thermograms recorded at $10^{\circ}\text{C min}^{-1}$ for quenched (Q) and annealed (A) iPP samples

Samples	T_1 ($^{\circ}\text{C}$)	T_3 ($^{\circ}\text{C}$)	ΔH_3 (J g^{-1})	X_c (%)
Q	64.0	162.6	83.0	60
A70	81.5	163.8	81.5	60
A93	100.8	162.8	85.0	62
A135	132.5	162.8	97.0	70
A160	—	172.0	117.5	85

higher temperatures. The sample annealed at 160°C exhibits only one endothermic peak (T_3). This could indicate that such an annealing results in the transformation of distorted microcrystallite into the lamellae of monoclinic habit exhibiting the largest size and/or the highest degree of perfection.

3.2. Wide-angle X-ray diffraction (WAXD)

Fig. 3 shows the wide-angle X-ray diffractograms of quenched (Q) and annealed (A) samples for 10 min at 70, 93, 135 and 160°C .

The as-received sample (Q) displays the well-known X-ray diffractogram usually observed for quenched isotactic polypropylene film [17, 23–26], i.e. two broad reflection profiles at $2\theta = 15^{\circ}$ and 21° . This X-ray spectrum differs from that recorded for isotactic polypropylene crystallized under the usual conditions [13, 23, 25]. In fact, α and β phases show respectively, four and five main well-defined reflection profiles in the same analysis angular range.

Thus, the two broad X-ray diffraction peaks exhibited by the quenched iPP film could result from the widening and overlapping of the main different peaks related to the monoclinic [11] and/or the hexagonal phases [28]. Such a broadening of the characteristic X-ray peaks of the monoclinic and/or the hexagonal phases observed in quenched iPP film could result from the two following origins: (i) the small size of the crystallites according to the well-known Debye–Scherrer equation in which the mean crystallite size is inversely related to the width at half-height of the reflection profile; and (ii) the lattice distortions because these crystalline entities are very distorted crystals showing an intermediate order between glass and crystalline phases.

Then, as suggested by Vittoria [23], the reciprocal of the half-height of the diffraction peak ($1/A$) located at about 15° (2θ) is chosen as a reliable parameter to evaluate both the size and perfection degree of crystallites, i.e. ($1/A$) increases with increasing size and/or perfection degree.

Table III lists the characteristic parameter values obtained from diffractom analysis for quenched and annealed samples. The ($1/A$) value determined for the sample annealed at 70°C is equal to that of the quenched specimen.

It can be noted in Fig. 3 that the diffractogram patterns displayed by the quenched and annealed sample at 70°C are similar. On increasing the annealing temperature to above 70°C , a clear resolution of the doublet in four diffraction peaks can be observed. As shown in Fig. 4, the ($1/A$) parameter is progressively increased on increasing the annealing temperature

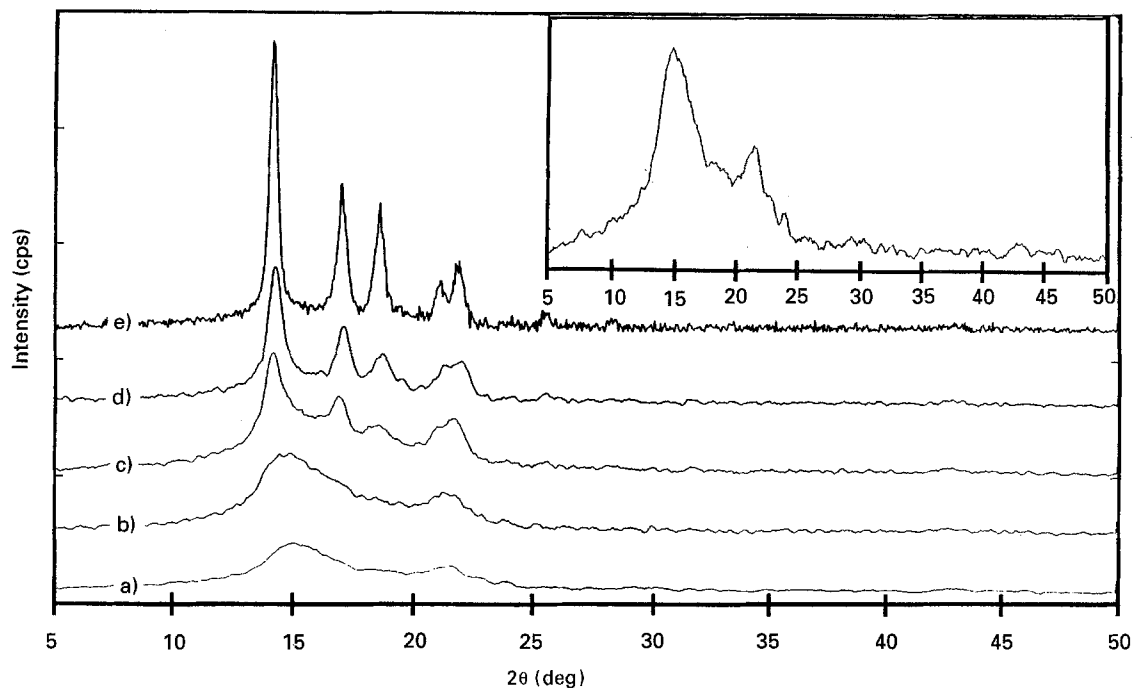


Figure 3 Wide-angle X-ray diffractograms displayed by (a) quenched iPP, and samples annealed for 10 minutes at (b) 70°C, (c) 93°C, (d) 135°C and (e) 160°C. Inset: an enlargement of the X-ray diffractogram of quenched iPP.

TABLE III Characteristics values determined for diffractograms displayed by quenched (Q) and annealed (A) samples at various temperatures 70, 93, 135 and 160°C

Samples	Locations of the diffraction profiles, 2θ (deg)				$\left(\frac{1}{A}\right)$ (deg ⁻¹)
Q	15.3	21.3	—	—	0.28
A70	15.0	21.4	—	—	0.28
A93	14.1	16.9	18.6	22.0	0.64
A135	14.1	17.1	18.7	21.3	1.23
A160	14.1	17.1	18.8	21.3	1.78
Monoclinic ^a	14.0	17.0	18.8	21.3	—
Structure (h, k, l)	(110)	(040)	(130)	(111)	

^a The characteristic parameters of the monoclinic form of the isotactic polypropylene are given for comparison [42].

from 70°C to 160°C. In agreement, with Vittoria [23–26], this could indicate the appearance of a crystalline phase of a monoclinic kind. The locations of diffraction peaks displayed by annealed samples almost superimpose those shown by the monoclinic phase of isotactic polypropylene [33, 42].

Thus, on increasing the annealing temperature from 70°C to 160°C, WAXD experiments provide evidence for an increase in the size and/or the degree of perfection of the crystalline entities. The sample annealed at 160°C shows the more perfect crystalline phase.

3.3. Density measurements

Fig. 5 shows the evolution of the density of samples versus the annealing temperature. Density first linearly increases on increasing the annealing temperature from 20°C (quenched sample) to 135°C and then exhibits an increase for an annealing temperature of 160°C. As crystallinity ratios of samples annealed at 70 and 93°C

are equal to that displayed by the quenched sample, we can deduce that the weak increase in density found for such annealed samples could result from an increase in the degree of perfection of the crystalline phase. The significant increase in density determined for the samples annealed at 135 and 160°C could result from the increase in both the crystallinity ratio and the degree of perfection of the crystallites.

Thus, according to WAXD, DSC and density measurements, the microstructure of quenched and annealed iPP films can be discussed as follows.

(i) Quenched iPP film and samples annealed at 70°C are both biphasic materials, i.e. an amorphous phase reinforced by distorted microcrystallites. Moreover, from DSC and density measurements, it can be concluded that the size and/or degree of perfection of microcrystallites of the annealed sample are higher than those of the crystalline entities of quenched iPP film.

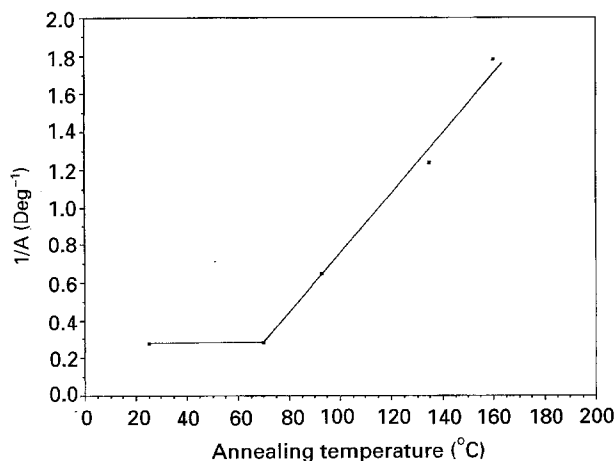


Figure 4 Evolution of the order parameter ($1/A$) versus the annealing temperature.

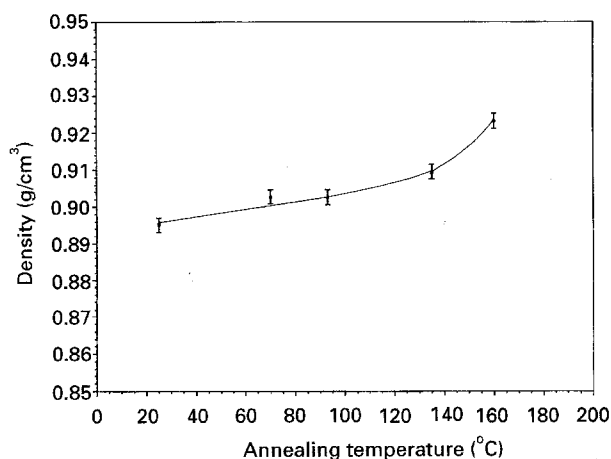


Figure 5 Evolution of the density of the analysed samples versus the annealing temperature.

As no significant change in the ($1/A$) parameter was detected for the annealed sample at 70°C from WAXD experiments, it can be suggested that the growth and increase in degree of perfection of microcrystallites could occur in a direction different from the c -axis [43].

(ii) The sample annealed at 160°C, exhibiting a significant increase in the crystallinity ratio with respect to other samples, is also a two-phase material, i.e. an amorphous phase reinforced by thick crystallites of monoclinic habit which exhibit a high degree of perfection.

(iii) From WAXD experiments, it could be suggested that samples annealed at 93 and 135°C exhibit an intermediate microstructure of the crystalline phase between that displayed by the quenched iPP film (and sample annealed at 70°C) and that shown by the sample annealed at 160°C. In fact, diffractograms recorded for the samples annealed at 93 and 135°C provide evidence for four diffraction peaks, as in the sample annealed at 160°C, but the reflection profiles are very large. Therefore, such annealed samples could be assumed to be either three-phase materials, i.e. an amorphous phase–distorted microcrystallites–crystallites of monoclinic habit, or two-phase systems, i.e. an

amorphous phase reinforced by microcrystallites, the size and degree of perfection of which are significantly higher than those displayed by the quenched iPP film and the sample annealed at 70°C.

According to the above discussion, it can be concluded that the crystallinity ratio can be accurately determined from density measurements for only the quenched iPP film and the sample annealed at 160°C. In fact, the crystallinity ratio, X_c , of such biphasic materials, is determined from the following equation

$$X_c = \frac{d_c}{d} \left(\frac{d - d_a}{d_c - d_a} \right) \quad (2)$$

where d is the measured density of the analysed sample, d_a is the density of the amorphous phase equal to 0.856 g cm⁻³ [23–26], and d_c is the density of the crystalline phase. For monoclinic phase and paracrystalline (or microcrystallites) phase, d_c is taken, respectively, equal to 0.936 and 0.916 g cm⁻³ [25]. The crystallinity ratios of the quenched iPP films and the sample annealed at 160°C are 67% and 85%, respectively.

For samples annealed at intermediate temperatures, X_c cannot be determined accurately from density measurements, as described above, because the density of the crystalline phase, d_c , progressively increases from 0.916–0.936 g cm⁻³ with increasing annealing temperature.

3.4. Dynamic mechanical spectrometry (DMS)

An original and complementary method to those previously used to characterize the microstructure of semicrystalline polymers is the dynamic mechanical spectrometry (DMS) carried out in the glass temperature range of such polymers. Such an experimental technique could furnish information on the microstructure of the amorphous phase assessed in terms of molecular motion ability of the macromolecular chains. Isochronal spectra of quenched iPP film and samples annealed at 70, 93, 135 and 160°C are recorded on increasing the temperature at 0.5°C min⁻¹ and at three frequencies 1, 5 and 10 Hz.

For example, the isochronal spectra recorded at 10 Hz for the quenched iPP film are shown in Fig. 6. For the three frequencies, dynamic mechanical spectra show a well-defined relaxation located at about 15°C. A drop in modulus is associated at such a $\tan \delta$ maximum. In agreement with Hsu *et al.* [14] and Cerere *et al.* [44], such a mechanical relaxation is related to the glass transition, T_g , of quenched iPP film. We recall that T_g was not detected from DSC experiments. Moreover, at about 70°C, a less-defined maximum of $\tan \delta$ can be seen, which could be related to the transitions occurring in the crystalline phase.

Fig. 7 shows isochronal $\tan \delta$ spectra recorded at 10 Hz for the samples annealed at the different temperatures. The $\tan \delta$ spectrum of quenched iPP films is given as reference. The annealed samples do not display the weak maximum of $\tan \delta$ observed for the quenched film.

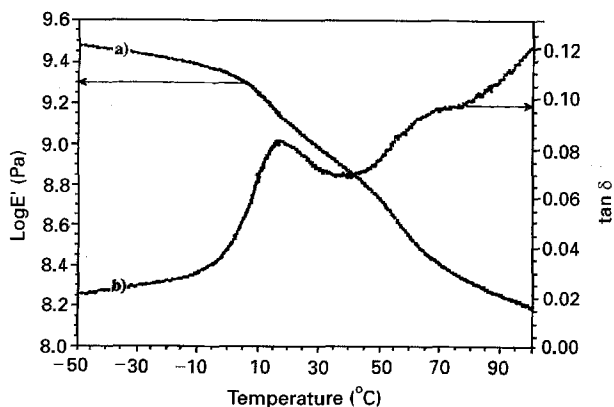


Figure 6 Plots of (a) $\log E'$ and (b) $\tan \delta$ versus temperature at 10 Hz for quenched iPP film.

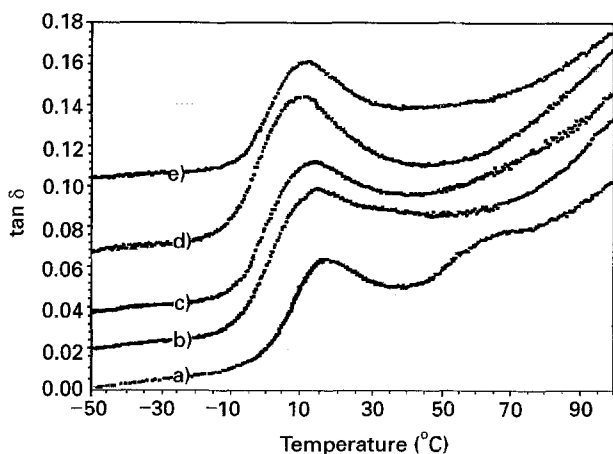


Figure 7 Isochronal $\tan \delta$ spectra recorded at 10 Hz for (a) quenched iPP films, and samples annealed at (b) 70 °C, (c) 93 °C, (d) 135 °C and (e) 160 °C.

Changes in microstructure of the amorphous phase induced on increasing the annealing temperature can be assessed through the determination of the following parameters:

- (i) the temperature location of the $\tan \delta$ maximum for a given frequency;
- (ii) the apparent activation energy, E_a , of the mechanical relaxation related to T_g , which can be assessed in a first approximation from the well-known Arrhenius law

$$f_T = f_0 \exp\left(-\frac{E_a}{RT}\right) \quad (3)$$

where f_T is the frequency of the $\tan \delta$ maximum curve at temperature T , and f_0 is the pre-exponential factor. In spite of the fact that the frequency dependence of the mechanical relaxation related to T_g obeys rather a WLF equation, i.e. the activation energy varies with temperature, such an Arrhenius law allows evaluation of an apparent activation energy in a given temperature range;

(iii) the magnitude of the mechanical relaxation, I_R , is assessed through the determination of the area under the $\tan \delta$ peak recorded at 10 Hz. Such an area is determined after subtracting the baseline taken as a straight line tangent to the right and the left side

TABLE IV Characteristic values determined from isochronal spectra for quenched (Q) and annealed (A) samples at 70, 93, 135 and 160 °C

Samples	$T_{\tan \delta \max}^a$ (°C)	E_a^b (kJ mol ⁻¹)	I_R^c (Arb. units)
Q	17.0	470	0.33
A70	14.5	385	0.83
A93	12.5	370	0.77
A135	10.0	320	0.76
A160	10.0	300	0.50

^a $T_{\tan \delta \max}$ temperature of the maximum in $\tan \delta$ at 10 Hz.

^b E_a , apparent activation energy.

^c I_R , magnitude of the $\tan \delta$ spectrum at 10 Hz.

minima preceding and following the $\tan \delta$ peak. I_R is expressed in arbitrary unit.

Table IV lists the values of such characteristic parameters determined for quenched iPP film and annealed samples. On increasing the annealing temperature from 20 °C to 160 °C, the main changes in characteristics of the mechanical relaxation related to T_g are:

- (i) the $\tan \delta$ maximum recorded at 10 Hz is progressively shifted towards the lower temperatures from 17 °C to 10 °C;
- (ii) the apparent activation energy decreases from 470 kJ mole⁻¹ to 300 kJ mole⁻¹;
- (iii) the magnitude of the mechanical relaxation, I_R , passes through a maximum (0.83 arb. units) for the sample annealed at 70 °C.

Such changes in the characteristics of the mechanical relaxation related to T_g can be interpreted in terms of modification of molecular mobility of chains in the amorphous phase, i.e. changes in the physical cross-linking degree of the amorphous phase by the crystalline phase.

Thus, based on the previous microstructural analysis performed by DSC and WAXD techniques, such changes in the physical cross-linking of the amorphous phase can be discussed as follows.

(i) As-quenched iPP film and samples annealed at 70 and 93 °C exhibit the same crystallinity ratio; the increase in the magnitude of the relaxation accompanied by a shift of the mechanical relaxation towards the lower temperatures (and a decrease in the apparent activation energy) observed for both the annealed samples can be due to a strong decrease in the physical cross-linking degree of the amorphous phase displayed by such samples with respect to that of the quenched film. Such an effect could result from an increase in the size of the crystallites in annealed samples as suggested by DSC and WAXD experiments. In fact, crystallites act as physical ties for the amorphous phase [44–46] and an increase in their sizes (for a constant crystallinity ratio) leads to a decrease in the interactions between the two phases. It can be noted that the physical cross-linking degree of the quenched iPP film is the highest. This could confirm that the crystalline phase in such a sample could be constituted by crystalline entities of very low size.

(ii) In spite of the crystallinity ratios being the highest for the samples annealed at 135 and 160 °C, it can be noted that such annealed samples display a stronger shift of the $\tan \delta$ peak towards a lower temperature, accompanied by an increase in the magnitude of the relaxation (with respect to that of the quenched sample). This suggests that the increase in the crystallinity ratio characteristic of an enhancement of the reinforcement effect displayed by the annealed sample is strongly counterbalanced by the large size of the crystallites. Thus, this results in a decrease in the physical cross-linking degree of the amorphous phase in these annealed samples.

4. Conclusion

The microstructure of quenched isotactic and annealed iPP films was investigated by using differential scanning calorimetry (DSC), wide-angle X-ray diffraction (WAXD), density measurements, and dynamic mechanical spectrometry (DMS).

The crystallinity ratio, size and degree of perfection of the crystalline entities have been evaluated by DSC, WAXD and density measurements. Dynamic mechanical spectrometry has provided evidence for the physical cross-linking degree of the amorphous phase induced by the crystalline phase.

Thus, quenched iPP film is found to be a biphasic material, i.e. an amorphous phase strongly cross-linked by microcrystallites exhibiting small size and a very low degree of perfection.

On increasing the annealing temperature from 20 °C (quenched sample) to 160 °C, (i) the crystallinity ratio first remains constant for annealing temperatures up to 93 °C and then progressively increases, (ii) the size and degree of perfection of crystalline entities both increase. The sample annealed at 160 °C is a two-phase material composed of an amorphous phase reinforced by the largest crystallites of monoclinic habit. Samples annealed at 93 and 135 °C can be either a biphasic material, i.e. amorphous phase–crystalline entities, which tend to the monoclinic habit, or a three-phase system, i.e. amorphous phase–crystalline entities–crystallites, of monoclinic habit; (iii) the physical cross-linking degree of the amorphous phase by the crystalline phase progressively decreases.

Acknowledgements

This work was supported by Composite and the Rhône-Alpes Region for a financial support. We would like to thank Dr A. Thozet and R. Vera, Centre de diffractométrie Henri Longchambon-Lyon 1, for X-ray diffraction measurements.

References

1. D. R. MORROW, *J. Macromol. Sci. Phys.* **B3**(1) (1969) 53.
2. J. VARGA, *J. Mater. Sci.* **27** (1992) 2557.
3. Z. MENCIK, *J. Macromol. Sci.* **B**(6) (1972) 101.
4. G. NATTA, P. CORRADINI and M. CESARI, *Atti. Acad. Naz. Lincei Rend.* **21** (1956) 65.

5. R. J. SAMUELS and R. Y. YEE, *J. Polym. Sci. A*(2) **10** (1972) 385.
6. A. TURNER JONES, J. M. AIZLEWOOD and D. R. BECKETT, *Makromol. Chem.* **75** (1964) 134.
7. HISKOSAKA, *Jpn J. Appl. Phys.* **12** (1973) 1293.
8. B. LOTZ, S. GRAFF and J. C. WITTMAN, *J. Polym. Sci. Polym. Phys. Ed.* **24** (1986) 2017.
9. R. L. MILLER, *Polymer* **1** (1960) 135.
10. R. ZANNETTI, G. CELOTTI, A. FICHERA and R. FRANCESCONI, *Makromol. Chem.* **128** (1969) 137.
11. G. BODOR, M. GRELL and A. KELLO, *Faserforsch. Textil. Technol.* **15** (1964) 527.
12. D. M. GEZOWICH and P. H. GEIL, *Polym. Eng. Sci.* **8** (1968) 202.
13. P. B. McALLISTER, T. J. CARTER and R. M. HINDE, *J. Polym. Sci. Polym. Phys. Ed.* **16** (1978) 49.
14. C. C. HSU, P. H. GEIL, H. MIYAJI and K. ASAI, *ibid.* **24** (1986) 2379.
15. G. NATTA, *SPE J.* (1979) 377.
16. J. GREBOWICZ, I. F. LAU and B. WUNDERLICH, *Polym. Sci. Polym. Symp.* **71** (1984) 19.
17. M. GLOTIN, R. R. RAHALKAR, P. J. HENDRA, M. E. A. CUDBY and H. A. WILLIS, *Polymer* **22** (1981) 731.
18. P. J. HENDRA, J. VILE, H. A. WILLIS, V. ZICHY and M. E. A. CUDBY, *ibid.* **25** (1984) 785.
19. R. SARAF and R. S. PORTER, *Molec. Cryst. Liq. Cryst. Lett.* **2** (1985) 85.
20. P. CORRADINI, V. PETRACCCONE, C. DE ROSA and G. GUERRA, *Macromolecules* **19** (1986) 2699.
21. A. FICHERA and R. ZANNETTI, *Makromol. Chem.* **128** (1975) 137.
22. D. T. GRUBB and D. Y. YOON, *Polym. Commun.* **27** (1986) 84.
23. V. VITTORIA, *J. Macromol. Sci. Phys.* **B28** (1989) 489.
24. *Idem*, *J. Polym. Sci. Polym. Phys. Ed.* **24** (1986) 451.
25. *Idem*, *J. Mater. Sci.* **27** (1992) 4350.
26. V. VITTORIA and A. PERULLO, *J. Macromol. Sci.* **B25** (1986) 2671.
27. N. ALBEROLA, M. FUGIER, D. PETIT and B. FILLON, *J. Mater. Sci.* **30** (1995) in press.
28. J. A. GAILEY and R. H. RALSTON, *SPE Trans.* **4** (1964) 29.
29. A. FICHERA and R. ZANNETTI, *Makromol. Chem.* **176** (1975) 1885.
30. D. J. BLUNDELL, *Polymer* **28** (1987) 2248.
31. P. CEBE and S. D. HONG, *ibid.* **27** (1986) 1183.
32. N. ALBEROLA, *J. Mater. Sci.* **26** (1991) 1856.
33. B. WUNDERLICH, "Macromolecular Physics", Vol. 1 (Academic Press, New York, 1973) p. 549.
34. S. Z. D. CHENG, H. S. BU and B. WUNDERLICH, *Polymer* **29** (1988) 579.
35. S. H. RYU, C. G. GOGOS and M. XANTHOS, *ibid.* **32** (1991) 2449.
36. C. PASSINGHAM, P. J. HENDRA, M. E. A. CUDBY, V. ZICHY and M. WELLER, *Eur. Polym. J.* **26** (1990) 631.
37. Y. LEE, R. S. PORTER and J. S. LIN, *Macromolecules* **22** (1989) 1756.
38. S. S. CHANG, *Polym. Commun.* **29** (1988) 138.
39. R. ALAMO and L. MANDELKERN, *J. Polym. Sci. B Polym. Phys. Ed.* **24** (1986) 2087.
40. M. E. NICHOLS and R. E. ROBERTSON, *ibid.* **30** (1992) 305.
41. M. P. LATTIMER, J. K. HOBBS, M. J. HILL and P. J. BARHAM, *Polymer* **33** (1992) 3971.
42. G. NATTA, P. CORRADINI and M. CESARI, *Atti. Accad. Nazl. Lincei. Rend. Sci. Fis. Mat. et Nat.* **22** (1957) 11.
43. F. DE CANDIA, P. IANNELLI, G. STAULO and V. VITTORIA, *Coll. Polym. Sci.* **266** (1988) 608.
44. A. CECERE, R. GRECO and A. TAGLIALATELA, *Polymer* **33** (1992) 1411.
45. N. ALBEROLA, J. Y. CAVAILLE and J. PEREZ, *Eur. Polym. J.* **28** (1992) 935.
46. R. F. BOYER, *Rubber Chem. Technol.* **36** (1963) 1303.

Received 1 March
and accepted 27 July 1994